ACADEMIC PRESS

Available online at www.sciencedirect.com

SCIENCE DIRECT®

Journal of Sound and Vibration 265 (2003) 81–107

JOURNAL OF SOUND AND VIBRATION

www.elsevier.com/locate/jsvi

Force reconstruction: analysis and regularization of a deconvolution problem

E. Jacquelin*, A. Bennani, P. Hamelin

Laboratoire Mécanique Matériaux, Université Claude Bernard Lyon I, Domaine universitaire de la Doua, IUT A Gnie civil F-69622 Villeurbanne cedex, France

Received 21 May 2001; accepted 3 July 2002

Abstract

The reconstruction of force is considered by means of indirect measurements. This necessitates taking measurements from the impacted structure and then to deconvolve those signals from the impulse response function. More precisely, the purpose of the work described here is to analyze a deconvolution technique and to solve the problems which occur. Thus, it is highlighted that the associated deconvolution problem depends on the location of the measurement points: is it possible or not to reconstruct the impact force versus the location of this point. Numerical predictions are compared and validated with experiment. But, the deconvolution is a well-known ill-posed problem: the results are often unstable. This is why it is necessary to regularize the problem, which consists of adding a condition to the solution which does not appear in the initial problem. Some regularization methods are presented. Nevertheless, they necessitate the determination of a parameter; the difficulty is to calculate an appropriate value of this regularization parameter. The methods are successfully used to recover an experimental force.

1. Introduction

The determination of impact load history is necessary to design a structure. This step in the design process is often critical: it is not always possible to instrument the impactor (impact of a bird on a windscreen, for example). This means that the dynamic force must be recovered by the help of indirect measurements: the problem is then to deconvolve two signals.

Those investigations have interested many researchers. Doyle wrote several papers in which he has described a frequency domain method [1–3]. Gao and Randall [4] use a cepstral analysis: this

*Corresponding author. Tel.: +33-4-72-69-21-30; fax: +33-4-78-94-69-06.
E-mail address: jac@iuta12m.univ-lyon1.fr (E. Jacquelin).

0022-460X/03/$ - see front matter
doi:10.1016/S0022-460X(02)01441-4

can be viewed as an extension of a frequency technique in which the division is replaced by subtraction; this procedure is more and more used in the study of periodic excitations acting on systems. A large time window must be used, when the frequency domain deconvolution is used: this is a global method which is not limited to the elapse of the waves propagation time. That is a great disadvantage when a few components of the force must be recovered (early time problems). So, time domain deconvolution is then useful. Chang and Sun [5], Yen and Wu [6,7] for example, have preferred to work in the time domain. The method consists of recording a response $S(M,t)$ at M, which is often a strain; then, to recover the load $F(I,t)$ induced by an impact at I, by solving the following integral equation:

$$S(M,t) = \int_0^t G(I,M,t-\tau)F(I,\tau)\,\mathrm{d}\tau = G(I,M,t) \bigstar F(I,t), \tag{1}$$

where $G(I,M,t)$ is the impulse response function between the points M and I; $\bigstar$ is the convolution product. Then, the problem to solve is a deconvolution one. It is obvious that the transfer function identification must be done first: which is another problem.

To solve Eq. (1), a discrete problem must be generated by sampling the convolution integral equation (1). This leads to a system of algebraic equations:

$$[\mathbf{S}] = [\mathbf{G}][\mathbf{F}], \tag{2}$$

where $[\mathbf{G}]$ is the transfer matrix:

$$[\mathbf{G}] = \Delta t \begin{pmatrix} G(I,M,\Delta t) & 0 & & & 0 \\ G(I,M,2\Delta t) & G(I,M,\Delta t) & \ddots & & \\ G(I,M,3\Delta t) & G(I,M,2\Delta t) & \ddots & \ddots & \\ \vdots & \vdots & \ddots & \ddots & 0 \\ G(I,M,n\Delta t) & G(I,M,(n-1)\Delta t) & \dots & \dots & G(I,M,\Delta t) \end{pmatrix}$$

$$[\mathbf{S}] = [S(M,\Delta t), \dots, S(M,n\Delta t)]^{\mathrm{t}},$$

$$[\mathbf{F}] = [F(I,0), \dots, F(I,(n-1)\Delta t)]^{\mathrm{t}},$$

$f_e = 1/\Delta t$ is the sampling frequency.

A deconvolution is an inverse problem and is a well-known ill-posed problem: the $[\mathbf{G}]$ matrix is ill-conditioned and consequently [8]:

- the system defined by Eq. (2) can be numerically insolvable,
- if the solution of system (2) exists, it may be unstable with regard to a small disturbance, such as a noise.

Those difficulties are often hidden in the literature on dynamic reconstruction of loads, even if its presence is implicit. In this article, one will say that a force is recoverable if it is not necessary to modify the initial problem to obtain an acceptable solution: a direct solving of Eq. (2) is sufficient.

No article on deconvolution in dynamics deals with the parameters which influence the ill-conditioning and then the reconstruction of force. In this paper, the first purpose is to analyze the deconvolution problem. To do that, some experiments are performed on a target which can be modelled analytically. First, the analytical modelling excited with numerical force is used: thus,

the experimental noise is eliminated. Then the real device is used. Particularly, the effect of the measurement points location is highlighted.

The sensitivity of the response with regard to noise leads one to modify the initial problem to obtain a robust solution: this procedure is called regularization. Some articles [7,9] implicitly deal with the regularization by introducing a supplementary condition: the force must stay positive. This method is an interesting regularization one but is limited to the reconstruction of impact forces. In this article some more general regularization techniques are displayed. Those methods are mathematically well-proved and widely used in different fields of applied science [8]. The Tikhonov regularization [10,11], and the truncation regularization [12], which are particular cases of filter factor regularization method, are presented. The second main purpose of the article is to highlight the difficulty to determine the regularization parameter, even if some methods exist to calculate it.

2. The system studied

2.1. Experimental set-up

Experiments using a Al-5054 aluminium plate as a target are performed. This one is circular (radius $a = 205$ mm; thickness $h = 5$ mm), clamped, isotropic (Young's modulus, the Poisson ratio and density are $E = 70$ GPa, $v = 0.3$ and $\rho = 2700\ \mathrm{kg/m^3}$, respectively). The force is applied at I, the centre of the plate; the dynamic response is recorded by two strain gages fixed at 1 cm (M_1) and 5 cm (M_5) from the centre of the plate. The test set-up has been chosen in order to obtain an analytical expression of the transverse displacement.

Data acquisition and analysis are made with a DSPT analyzer (Siglab 20-42). Experimental frequency response functions (FRF) are obtained by impulse testing performed with an impact hammer (B&K 8202).

2.2. Analytical modelling

The system is modelled by an elastic, circular embedded "Kirchhoff" plate with uniform characteristics, subjected to axisymmetrical load acting on its centre. The equation of motion can be expressed in the following form [13]:

$$D\Delta\Delta w(r,t) + \rho h\ddot{w}(r,t) = q(r,t), \tag{3}$$

where $w(r,t)$ is the transverse displacement, $q(r,t) = f(t)\delta(r)$ the applied loading at the centre of the plate, $D = Eh^3/12(1-v^2)$, and $\Delta = (1/r)\mathrm{d}/\mathrm{d}r(r\,\mathrm{d}/\mathrm{d}r)$.

It is well-known [13] that the mode shapes of such a plate under axisymmetrical loading are:

$$\phi_n(r) = \mathrm{J}_0(\lambda_n r) - \frac{\mathrm{J}_0(\lambda_n a)}{\mathrm{I}_0(\lambda_n a)}\,\mathrm{I}_0(\lambda_n r),$$

where J_p and I_p are p order first kind and first kind modified Bessel's functions, respectively; λ_n is such as $\lambda_n^4 = \omega_n^2\rho h/D$ and is a solution of the following characteristic equation:

$$\mathrm{J}_0(\lambda_n a)\mathrm{I}_1(\lambda_n a) + \mathrm{I}_0(\lambda_n a)\mathrm{J}_1(\lambda_n a) = 0. \tag{4}$$

By applying the modal superposition, the displacement $w(r,t)$ can be expressed in the following form:

$$w(r,t) = \sum_n \frac{1}{M_n \omega_{an}} \int_0^t \phi_n(0)\phi_n(r) f(\tau) \sin(\omega_{an}(t-\tau)) \exp(-\xi_n \omega_n (t-\tau))\, \mathrm{d}\tau, \tag{5}$$

where M_n, ω_n, ω_{an} and ξ_n are modal mass, circular eigenfrequency, damped circular eigenfrequency ($\omega_{an} = \omega_n\sqrt{1-\xi_n^2}$) and the damping ratio for the eigenmode n.

In this study, the strains in the circumferential direction ε_t, on the surface of the plate ($z = h/2$) are recorded:

$$\varepsilon_t(r, h/2, t) = -\frac{h}{2r}\frac{\mathrm{d}w}{\mathrm{d}r}(t).$$

Then the modal expansion of the impulse response function between the centre of the plate ($r = 0$) and a measurement point located at r can be deduced:

$$G_t(r,0,t) = -\frac{h}{2r} \sum_n \frac{\phi_n'(r)\phi_n(0) \sin(\omega_n\sqrt{1-\xi_n^2}t) \exp(-\xi_n\omega_n t)}{M_n\omega_n\sqrt{1-\xi_n^2}}. \tag{6}$$

2.3. Excitations

Two kinds of excitation will be used:

- *Numerical force*: A numerical impact force represented in Fig. 1 is built. It is then possible to find the response at any position of the plate by applying Eq. (1), i.e., a forward problem. It is worth noting that the numerical force is well-known and not spoiled by any noise.
- *Actual force*: A force obtained with an impact hammer is recorded. Simultaneously, the strains induced by the solicitation are recorded (Fig. 2).

3. Analysis of the deconvolution problem

3.1. Recoverable force?

In this section, the ability to solve Eq. (2) is studied. Then, a forward problem is carried out: both matrices $[\mathbf{G}_{t1}]$ and $[\mathbf{G}_{t5}]$ are multiplied by the numerical force $[F]$ and then the strains $[\varepsilon_{t1}]$ and $[\varepsilon_{t5}]$ are obtained. The problem is: can an inverse problem be performed, i.e., can the force $[\mathbf{F}]$ be recovered? The response is positive if the solution of the linear algebraic system (2) is exactly the initial force: the problem is then to determine if a small disturbance leads to a small variation of the solution or not.

Indeed, the whole simulations show that the conclusion is a function of the location of the measurement point. Thus, if the results can perfectly be recovered with the strains measured at 1 cm from the centre (Fig. 1), it is not the same with the point located at 5 cm: the solution is

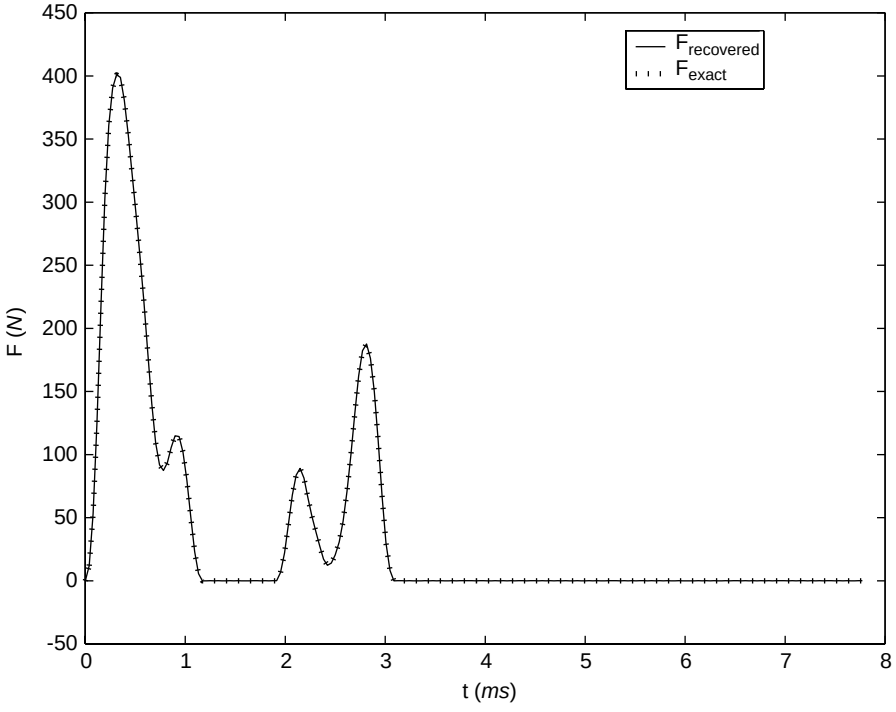

Fig. 1. Numerical impact force—Recovered force—measurement point at 1 cm.

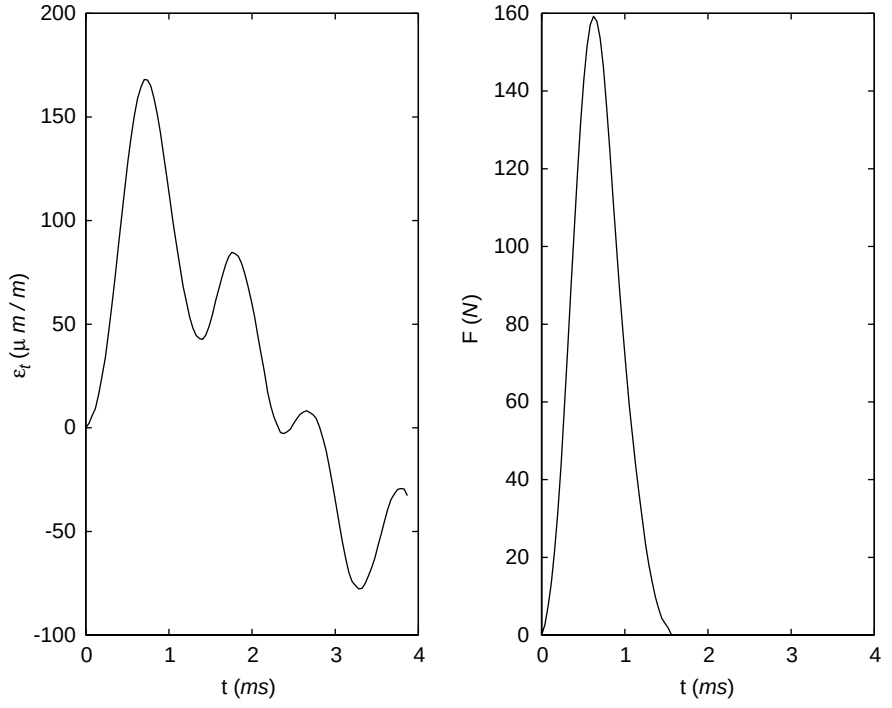

Fig. 2. Instrumented test: strain and force.

divergent. Then, it seems that the nature of the deconvolution problem is not the same in both cases.

3.2. Nature of the deconvolution problem

A useful tool will help one to prove that the nature of the deconvolution problem depends on the point measurement location: the singular value decomposition (SVD). The SVD of a $[\mathbf{G}]$, (m,n), $m \geqslant n$, real matrix is defined as follows:

$$[\mathbf{G}] = [\mathbf{U}][\mathbf{\Sigma}][\mathbf{V}]^{\mathrm{t}} = \sum_{i=1}^{n} u_i \sigma_i v_i^{\mathrm{t}}, \tag{7}$$

where $[\mathbf{U}]$ is the matrix of left singular vectors, $[\mathbf{V}]$ is the matrix of right singular vectors and $[\mathbf{\Sigma}]$ diagonal matrix whose diagonal elements are the singular values of $\mathbf{G}$.

This decomposition is particularly interesting because it gives a formulation of the solution of problem (2):

$$[\mathbf{F}] = \sum_{i=1}^{n} \frac{\mathbf{u}_i^{\mathrm{t}}[\mathbf{S}]}{\sigma_i} v_i. \tag{8}$$

Then the ability to solve system (2) depends on the singular values and vectors of the matrix $[\mathbf{G}]$.

Moreover, the singular values will help one to determine the nature of the problems. Indeed, if a discrete equation leads to ill-conditioned matrices, there exists different kinds of ill-conditioning [12]: the problem can be solely ill-posed or can be ill-posed and rank-deficient.

The nature of an ill-conditioning is identified with the singular values well:

- the singular values decay gradually to zero with no particular gap: the problem is only ill-posed,
- the singular values decay gradually to zero and there is a well-determined gap between two singular values: the problem is ill-posed and "rank-deficient". Moreover, the SVD allows one to identify the pseudo-rank of the matrix: it is the number of singular values which appear before the gap.

In Fig. 3, the singular values of the matrices $[\mathbf{G}_{t1}]$ and $[\mathbf{G}_{t5}]$ are plotted. This figure shows that the nature of the problem changes with the position of the measurement point:

- the inverse problem posed with $[\mathbf{G}_{t1}]$ is solely ill-posed,
- the inverse problem posed with $[\mathbf{G}_{t5}]$ is ill-posed and rank-deficient.

Expression (8) and Fig. 3 explain why it is impossible to recover the force with the matrix $[\mathbf{G}_{t5}]$: the smallest singular value (10^{-24}) is below the computer precision (10^{-16}), therefore the results are dominated by rounding errors and it is impossible to recover the force; that is not the case with $[\mathbf{G}_{t1}]$.

Experimental verification: The previous conclusions are made from some numerical signals and modelling and it would be interesting to validate them from experimental data. So, the experimental frequency response functions are determined; by inverse Fourier transform, the impulse response function are obtained and finally the transfer matrices $[\mathbf{G}_{t1}]$ and $[\mathbf{G}_{t5}]$ are

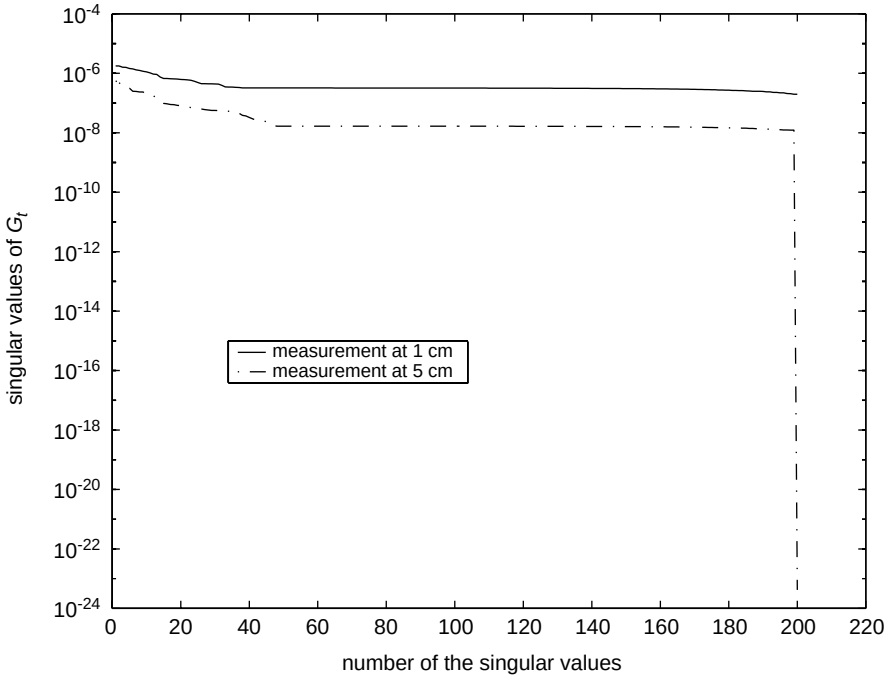

Fig. 3. $[G_{t1}]$ and $[G_{t5}]$ singular values.

performed by sampling. To test if it is possible to reconstruct the impact force, the signals previously described are used (Fig. 2).

Then, the discrete convolution problem (2) is solved. The solution allows one to conclude if the impact force is recoverable: Fig. 4 shows that only the measurements at 1 cm allow the reconstruction, according to the numerical results. This validates the influence of the measurement point location.

Moreover, the SVD proves that the problem is rank-deficient and very ill-conditioned if the measurement point located at 5 cm is used (Fig. 5).

3.3. Solution existence of a deconvolution problem

A lower triangular matrix [**G**] is involved in the discrete convolution problem (2)

$$[\mathbf{S}] = [\mathbf{G}][\mathbf{F}]. \tag{9}$$

Then, the force can be recovered sequentially by a direct solution. But, it is not so simple because simultaneity is involved Eq. (2). In practice, there is not simultaneity between the force and its effect at any point of the structure: that is due to the elapse of the propagation time of the waves. Then, some of the first rows of [**G**] are filled with zeros: the problem is rank-deficient and then under-determined.

Fig. 6 effectively shows the delay between the transient signals measured at 1 and 5 cm. In that example, the delay is $t_d = 132$ μs and the time sampling is $\Delta t = 39$ μs. Then, the index delay is

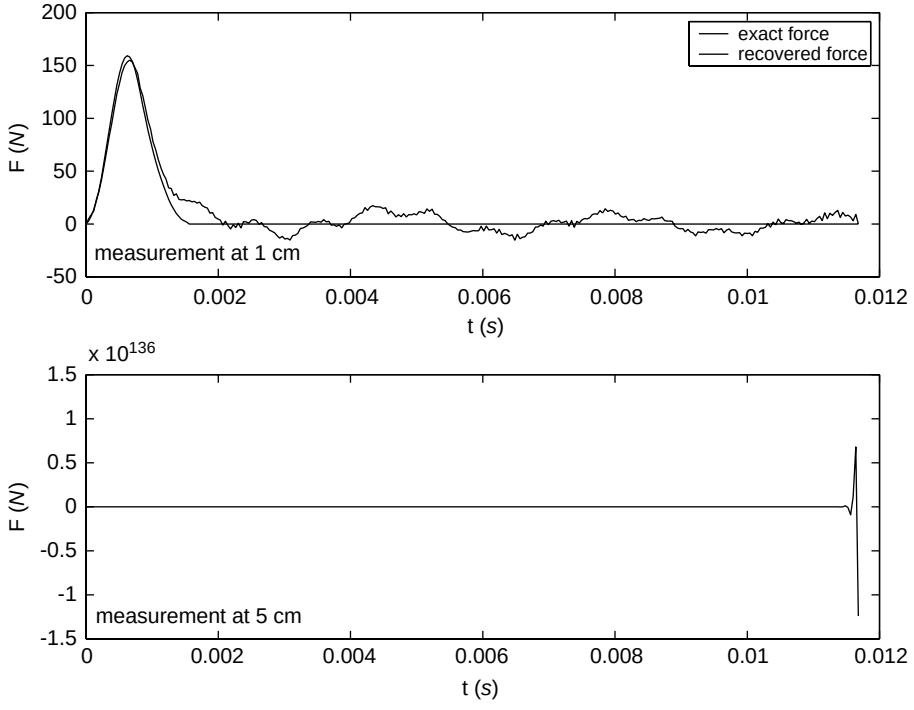

Fig. 4. Force reconstruction with experimental data.

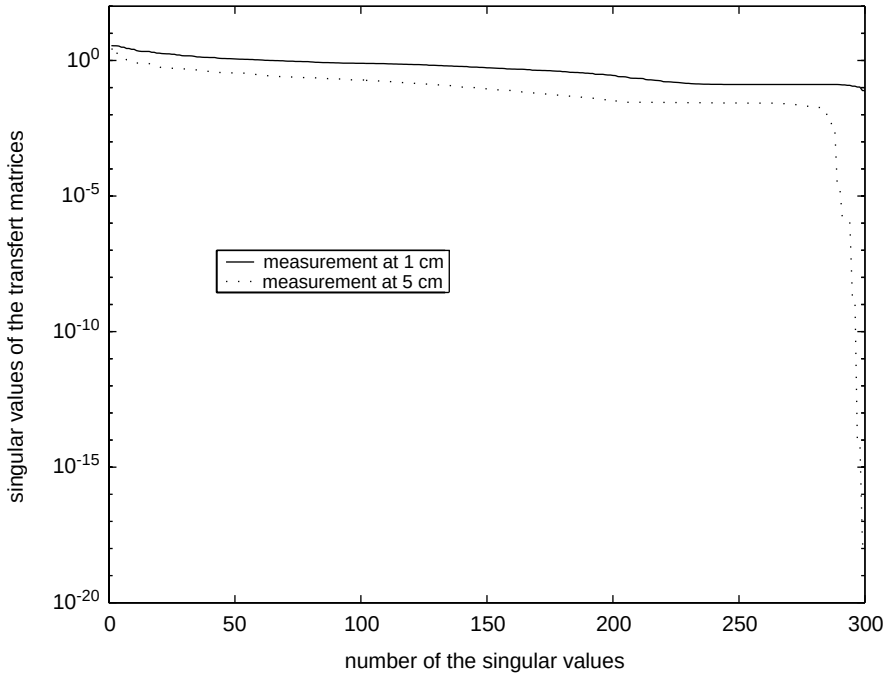

Fig. 5. Singular values of the experimental transfer matrices.

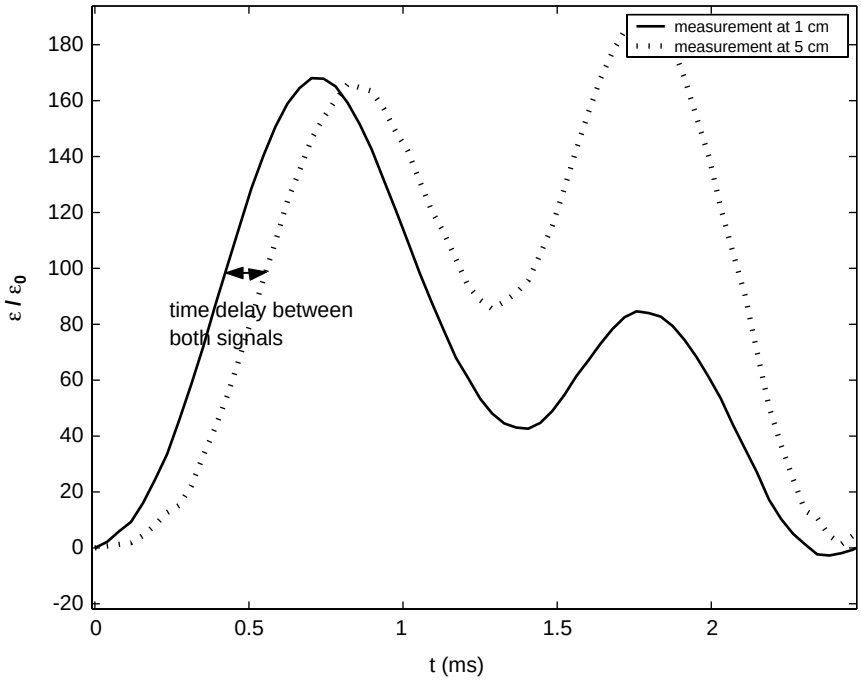

Fig. 6. Time delay induces by the wave propagation.

$n_d = t_d/\Delta t \sim 3$. As the signals are recorded at 1 and 5 cm from the point of excitation, there is an almost simultaneity between the force and the signal recorded at 1 cm, and a delay $(4 \times \Delta t)$ between the force and the signal recorded at 5 cm. This can explain why only the latter problem is rank-deficient.

It may be interesting to know if the force becomes recoverable by keeping only the singular values before the gap in expression (8): the SVD is then truncated. Indeed, if the solution is not divergent, some disturbing oscillations appear in the solution. This is due to a propriety of the singular vectors: they present more and more oscillations when the index i increases, exactly as if those vectors represent the high frequency components of the solution [12]. Then, if the coefficients of the last retained vectors are not sufficiently small, those oscillations are highlighted. In the following, it will be seen that it is possible to obtain a good solution by a truncation of the SVD: the problem is then to determine the "good" rank of the truncation. Then, one substitutes a well-posed problem closed to the rank-deficient problem: this technique is a regularization one.

Moreover, the solution depends also on n, the number of time steps: if this latter is sufficiently small, the singular values are not below the computer precision. Thus, the Table 1 shows that the smallest singular values are not less that the computer precision when the number of time step is 200: in that case, the force is recoverable. But, as shown in Table 1, if the size of the problem increases, i.e., if the total number of time steps increases (up to 800 for example), the solution becomes divergent: the lowest singular value depends strongly on the number of time

Table 1
Some singular values of different FRF

Number of time steps	G_{r5}		G_{t1}	
	Lowest singular value	Greatest singular value	Lowest singular value	Greatest singular value
200	2.8×10^{-7}	4.3×10^{-6}	2.8×10^{-7}	2.1×10^{-6}
800	10^{-24}	10^{-15}	3.5×10^{-8}	6.4×10^{-6}

steps for the measurement at 5 cm. Then, if a small sampling period is required for a forward problem to obtain some accurate results, this could induce an impossibility to solve the inverse solution.

3.4. Solution stability of a deconvolution problem

Between a numerical simulation and an experimental test, there is a great difference: in the latter case, the impulse response function and the output signals are noisy. Then, even if a non-divergent solution of the deconvolution problem can be obtained, it is important to test its stability, because the problem is ill-conditioned. More particularly, for a given noise level, when the sampling period decreases, the solution is spoiled by a severe oscillation. Indeed, the errors are amplified and propagate when an ill-conditioned system is solved: that creates a parasitical oscillation which becomes larger when the number of discrete time steps increases. In fact, the convolution of a force by an transfer function has a smoothing effect [8,14]. Then, a rather important oscillation of the force can induce a small effect on the result.

To test the influence of the noise, modelled by a zero-mean gaussian random process:

- a deterministic forward problem is performed: a strain is obtained by convolving the numerical force and the analytical impulse response function,
- a signal is disturb; it can be:
  – either the output response (noise measurement): the standard deviation is 1.5% of the maximum of the measured strains,
  – or the impulse response (modelling noise): the standard deviation is 1% of the maximum of the impulse response function.
- an inverse problem is performed by directly solving the algebraic system (2). A measure of the discrepancy $\mathscr{D}$ between the both exact and noisy force is defined by the following relation:

$$\mathscr{D} = \frac{\|Signal_{noisy} - Signal_{exact}\|}{\|Signal_{exact}\|}. \tag{10}$$

The term "exact" is applied for the signals without any noise.

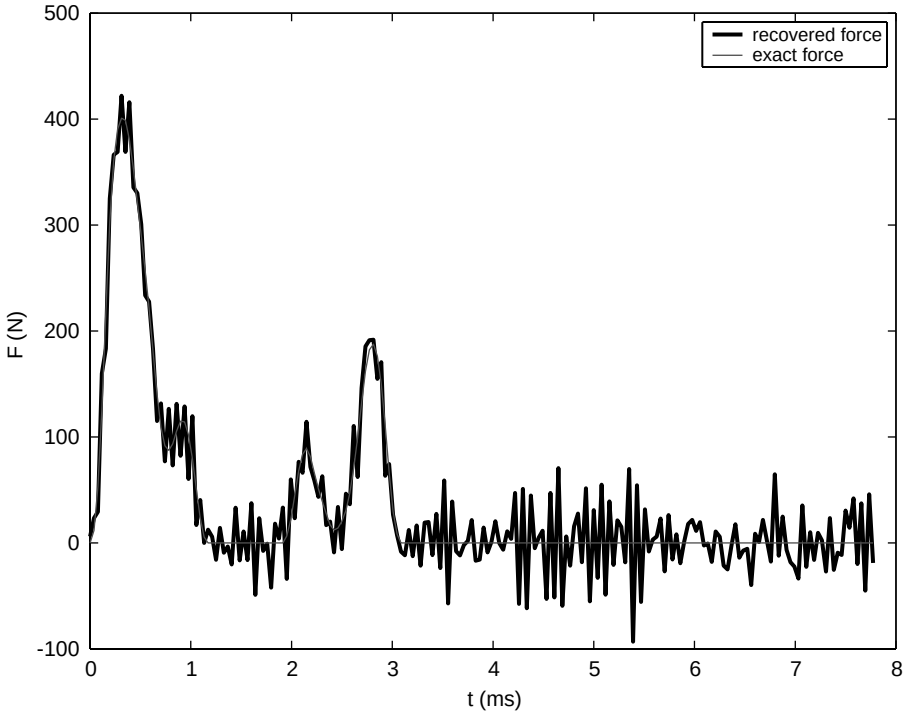

Fig. 7. Force recovered from noisy response.

Previously, it has been shown that it is possible to recover the force if a measurement point at 1 cm is used: in this subsection, all the calculations are performed with the response recorded at this point.

The results are function of the nature of the noise:

- *Noisy response*: In Fig. 7, the recovered force is plotted when the noisy strains are used. The error $\mathscr{D}$ calculated with formula (10) is 5% for the output response; this error induces an error of 30% on the solution. Then, even if the measurement at 1 cm allows to recover the force with perfect data, as soon as there exists some noise, it is not possible to obtain a correct force: the solution is unstable.
- *Noisy impulse response function*: Contrary to the previous results, the influence of the noise on the structure characteristics is weak: 5% in error for impulse response function produces an 5% in error for the recovered force (Fig. 8).

In practice, the measured signal is always a noisy one. Then, one cannot accept the solution obtained by the direct solution of the discrete deconvolution equation. A regularization technique must also be used to stabilize the force. This technique imposes a smoothness on the solution: it forces neighbouring values to be almost similar.

Comment: The previous simulations highlight that the solution of an inverse problem is not acceptable by directly solving Eq. (2) as soon as the output response is noisy. It is worth noting

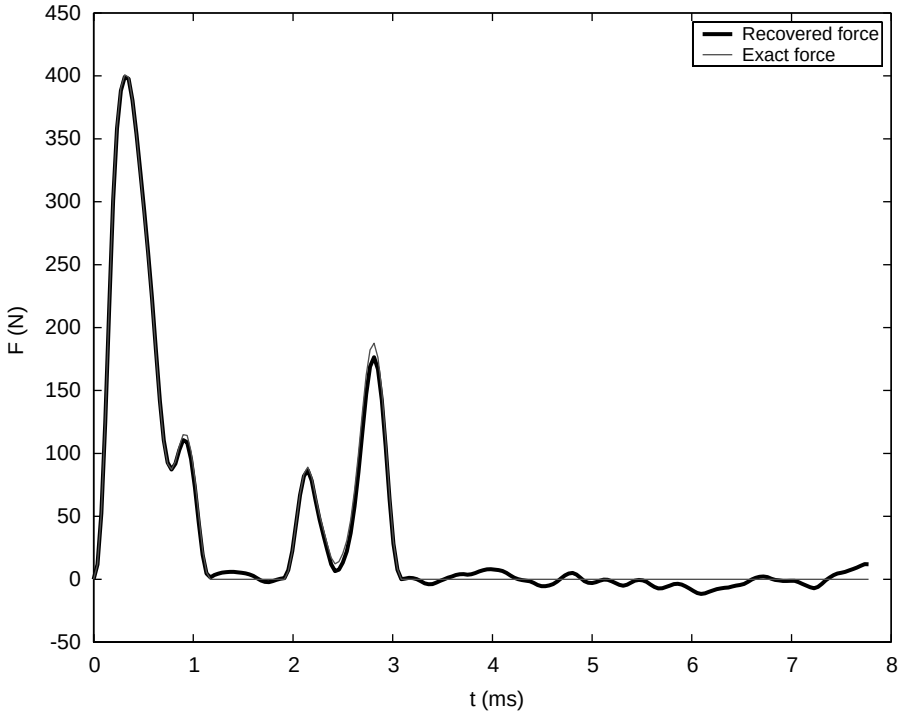

Fig. 8. Force recovered from noisy impulse response function.

that this conclusion is not the same as when a noisy impulse response is used. This explains why, in the literature, the quality of the results does not depend on the origin of the transfer matrix: it can be obtain either by modelling [6,9,15,16], or experiment [7,16].

4. Regularization

The main conclusion of the previous analysis is that the "naive" solving of the equation (2) never gives a satisfactory solution. Then, a regularization technique must be used; it allows one to:

- always recover the force, whatever the measurement position,
- obtain a stable solution with regard to the noise.

The regularization consists of including additional information to the initial problem. This additional condition can be:

- *Physical*: For example, when an impact force must be recovered, the solution is forced to be non-negative,
- *A compromise*: It might be a solution which minimizes the residual norm of the discrete convolution equation (2) and a smoothness condition on the solution (norm of the force or of its derivatives not too high, etc.).

4.1. Non-negativity condition

To recover an impact force, the regularization technique commonly used consists of adding a non-negativity condition. This one is particularly well-adapted because it is based on a physical consideration: there is no compromise. The deconvolution problem to solve is then:

$$\min_F \|[\mathbf{G}][\mathbf{F}] - [\mathbf{S}]\|_2 \text{ subject to } [\mathbf{F}] \geqslant 0. \tag{11}$$

This can be solve by the conjugate gradient method [17].

As shown before, the force is not recoverable if the point at 5 cm is used. If the non-negativity condition is applied, the exact force is obtained whatever the measurement point used. This conclusion is also valid when the strains are noisy (Fig. 9). Then, the regularization strongly stabilizes the solution but this condition of positivity cannot always be used: this is why the regularization with a compromise is presented to reconstruct any force in the following subsection.

4.2. Regularization with compromise

This method incorporates further information about the desired solution in order to stabilize the problem, which is not based on physical consideration. Then a regularized problem consists in finding a solution [**F**] such as

$$\min_F \|[\mathbf{G}][\mathbf{F}] - [\mathbf{S}]\|_2 \text{ subject to } \textit{further conditions}. \tag{12}$$

For the study, the knowledge and the solution of that regularized problem, it is interesting to use the generalized singular value decomposition (GSVD). This is why this tool is defined first, to use it widely afterwards.

The described methods will be illustrated with the numerical noisy signals used in the previous section to estimate the force plotted Fig. 1.

4.2.1. Generalized singular value decomposition GSVD [12]

Briefly, the GSVD of the real matrix pair ([**G**], [**L**]), ([**G**] $\in \mathbb{R}^{m\times n}$ and [**L**] $\in \mathbb{R}^{p\times n}$, $m \geqslant n \geqslant p$) is:

$$[\mathbf{G}] = [\mathbf{U}] \begin{pmatrix} [\mathbf{\Sigma}] & 0 \\ 0 & \mathbf{I}_{n-p.} \end{pmatrix} [\mathbf{X}]^{-1} = [\mathbf{U}][\mathbf{\Delta}][\mathbf{X}]^{-1},$$

$$[\mathbf{L}] = [\mathbf{V}]([\mathbf{M}], 0)[\mathbf{X}]^{-1},$$

where [**U**] is the $(\mathbf{u}_1, \ldots, \mathbf{u}_n)$ is an $m \times n$ matrix which has its columns orthonormal; [V] the $(\mathbf{v}_1, \ldots, \mathbf{v}_p)$ is an $p \times p$ matrix which has its columns orthonormal; [**X**] a non-singular $n \times n$ matrix; $[\mathbf{\Sigma}] = \text{diag}(\sigma_1, \ldots, \sigma_p)$ where $1 \geqslant \sigma_p \geqslant \cdots \geqslant \sigma_1 \geqslant 0$; $[\mathbf{\Delta}] = \text{diag}(\delta_1, \ldots, \delta_n)$ where $\delta_i = \sigma_i$ if $i \leqslant p$ and otherwise $\delta_i = 1$; $[\mathbf{M}] = \text{diag}(\mu_1, \ldots, \mu_p)$ where $1 \geqslant \mu_1 \geqslant \cdots \geqslant \mu_p \geqslant 0$; $\mu_i^2 + \sigma_i^2 = 1$, $\gamma_i = \sigma_i/\mu_i$ are the generalized singular values, $\mathbf{I}_{n-p}$ the identity matrix of $\mathbb{R}^{(n-p)\times(n-p)}$.

The solution in a least square sense of problem (2), can be obtain with the help of the GSVD:

$$[\mathbf{F}] = \sum_{i=1}^{p} \frac{\mathbf{u}_i^{\mathrm{t}}[\mathbf{S}]}{\sigma_i} \mathbf{x}_i + \sum_{i=p+1}^{n} \mathbf{u}_i^{\mathrm{t}}[\mathbf{S}]\mathbf{x}_i = [\mathbf{X}][\mathbf{\Delta}]^{-1}[\mathbf{U}]^{\mathrm{t}}[\mathbf{S}]. \tag{13}$$

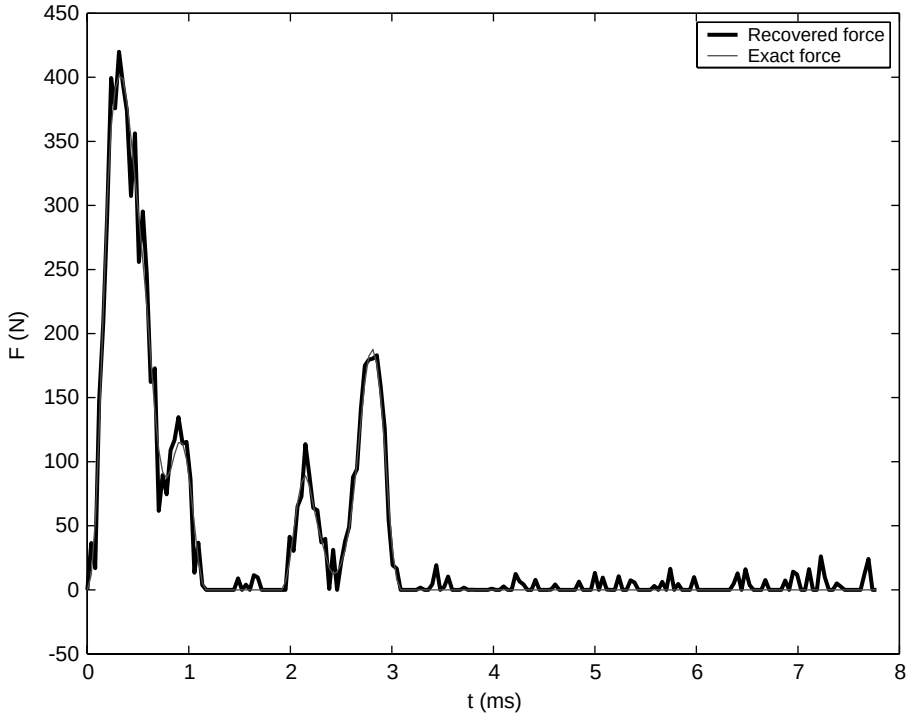

Fig. 9. Force recovered with a non-negativity condition and noisy strains measured at 5 cm from the centre.

Remark 1. This decomposition looks like the SVD. This is why some properties are similar to those of the SVD described previously, even if the ordering of the singular values and vectors is reversed. Thus, for ill-posed problem, the following features of the GSVD is usually found [12]:

- γ_i and σ_i decay to zero when i tends to 1,
- the singular $\mathbf{u}_i$, $\mathbf{v}_i$ and $\mathbf{x}_i$ are more and more oscillating as the corresponding γ_i decreases: they can be seen like some high frequency components of the signal.

Remark 2. The GSVD of $([\mathbf{G}], \mathbf{I}_n)$ and the SVD of $[\mathbf{G}]$ are identical except for the reverse ordering. The GSVD allows one to add more general conditions than the SVD: that is why it is so interesting to use the GSVD.

4.2.2. Filter factors

As it has be seen with the SVD, the ill-posedness is highlighted with the GSVD. Indeed, the previous Remark 1 and expression (13) indicate that the low index terms made the problem ill-conditioned:

- when i tends to 1, $1/\sigma_i$ tends to infinity: if $\mathbf{u}_i^t[\mathbf{S}]$ does not tend to zero faster than σ_i, the solution is unstable;

- when i tends to 1, $\mathbf{x}_i$ is oscillating: if the term $\mathbf{u}_i^t[\mathbf{S}]/\sigma_i$ does not tend to zero so quickly, the solution becomes strongly oscillating; this is why the high frequency components often pose a problem.

Then, the idea [12] is to modify the GSVD with the help of some parameters f_i called the filter factors:

$$[\mathbf{F}] = \sum_{i=1}^{p} f_i \frac{\mathbf{u}_i^t[\mathbf{S}]}{\sigma_i} \mathrm{x}_i + \sum_{i=p+1}^{n} \mathbf{u}_i^t \mathbf{S} x_i = [X][\boldsymbol{F}][\boldsymbol{\Delta}]^{-1}[\mathbf{U}]^t[\mathbf{S}] = [\mathbf{G}^\sharp][\mathbf{S}], \tag{14}$$

where $[\boldsymbol{F}]$ is a diagonal matrix: $[\boldsymbol{F}] = \mathrm{diag}(f_1, \ldots, f_p)$ and $\forall i = 1, \ldots, n-p$ $f_{p+i} = 1$, and $[\mathbf{G}^\sharp] = [\mathbf{X}][\boldsymbol{F}][\boldsymbol{\Delta}]^{-1}[\mathbf{U}]^t$ is a regularized pseudo-inverse of $[\mathbf{G}]$.

The filter factors goal is to minimize the influence of the low index terms: many expressions are available. Subsequently, two different filter factors will be presented, which correspond to two regularization techniques widely used:

- Tikhonov regularization,
- the truncation of the GSVD.

4.2.3. Tikhonov regularization [10]

The Tikhonov regularization consists in defining a smoothing norm $\Omega([\mathbf{F}])$ and finding a trade-off between the residual norm of Eq. (2) and the smoothing norm [10]. The regularized problem is then

$$\min_F \{\|[\mathbf{G}][\mathbf{F}] - [\mathbf{S}]\|_2\} \text{ subjected to } \min_F \{\Omega([\mathbf{F}])\}. \tag{15}$$

Typically, $\Omega([\mathbf{F}])$ is of the form

$$\Omega([\mathbf{F}]) = \|[\mathbf{L}][\mathbf{F}]\|_2, \tag{16}$$

where $[\mathbf{L}]$ is often the identity operator $(\mathbf{I})$, the first (D^1) or second (D^2) derivative operator,... $\Omega([\mathbf{F}])$ is a quadratic form whose matrix is a positive definite one: problem (15) is then a well-posed one and leads to a unique solution [14].

Tikhonov [10] has shown that this latter problem is equivalent to the following one:

$$\min_F \{\|[\mathbf{G}][\mathbf{F}] - [\mathbf{S}]\|_2 + \alpha\Omega([\mathbf{F}])\} \quad \text{and} \quad \Omega([\mathbf{F}]) = \|[\mathbf{L}][\mathbf{F}]\|_2, \tag{17}$$

where α is the regularization parameter. An important problem is the choice of α [12,18]: its value allows one to single out a minimum of the residual norm of Eq. (2) (low value) or a minimum of the smoothing norm (great value).

In fact, it can be shown that a solution of (17) is given by Eq. (14) with the following filter factors:

$$\forall i \leqslant p \; f_i = \frac{\gamma_i^2}{(\gamma_i^2 + \alpha^2)} \quad \text{if } [\mathbf{L}] \neq \mathbf{I}_n, \tag{18}$$

$$\forall i \leqslant p \; f_i = \frac{\sigma_i^2}{(\sigma_i^2 + \alpha^2)} \quad \text{if } [\mathbf{L}] = \mathbf{I}_n. \tag{19}$$

The latter expressions show that α is a really critical parameter: if it is too low, the problem stays unstable (its role is negligible); if it is too high the "high frequency" components are not taken into account, the solution is too smooth.

Indeed, the objective of the Tikhonov regularization is to modified only the terms of the GSVD which present a too small singular value.

Remark. To solve problem (15), the use of the GSVD is not the more efficient technique. For example, Granger [19,20] proposes a method to solve efficiently this problem. But, the GSVD allows one to understand the role of α and the principle of the Tikhonov regularization.

4.2.4. The truncation

Solution (13) shows that the problem of convergence is due to the low index terms of the decomposition. The truncation consists of eliminating the first terms up to the rank k. This index k is, in that method, the regularization parameter: it plays the same role as α in the previous method.

The index k must be chosen to eliminate:

- the small singular values,
- the too oscillating singular vectors.

The solution can again be written like expression (14), with the following filter factors:

$$f_i = 0 \quad \text{if } i \leqslant k, \tag{20}$$

$$= 1 \quad \text{otherwise.} \tag{21}$$

The truncation can be interpret as a traditional signal processing: one eliminates some high frequency components of the signal, which are the low index vectors $\mathbf{x}_i$.

4.2.5. Regularization parameter

The filter factors depend on a regularization parameter: the regularization quality is direct function of an adequate choice of this parameter. Unfortunately, these does not exist a universal method giving a good value for α or k.

The two following methods are often used, even if some others exist [10,19]:

- the L-curve,
- the generalized cross-validation (GCV).

L-curve criterion: To obtain the L-curve, one plots on a log–log scale the smoothing norm $\|[\mathbf{L}][\mathbf{F}]\|_2$ versus the residual norm of Eq. (1), $\|[\mathbf{G}][\mathbf{F}] - [\mathbf{S}]\|_2$: then, this is a curve parametrized by the regularization parameter (Fig. 10) which looks like an "L": it presents an horizontal and a vertical branchs linked at the "corner" of the curve. It illustrates the compromise

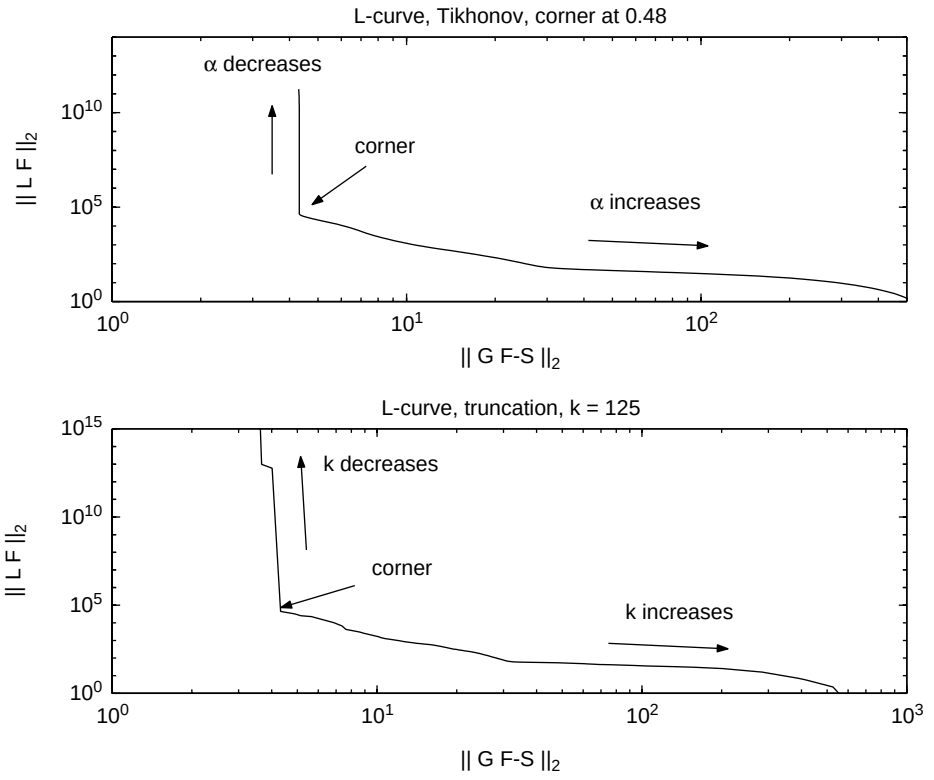

Fig. 10. L-curve $-L = D^2$.

between fitting the data well and to sufficiently regularize the solution. Thus, if the value of the parameter is:

- "small": the quality of the fit is good but the additional information is not take into account; the solution obtained is an oscillating (under-smoothing) one (Fig. 11);
- "high": the a priori condition is used well, at the cost at the fit: the solution is over-smoothing (Fig. 11).

The L-curve criterion indicates that the appropriate values are obtained for the points which are located at the corner of the curve.

Generalized cross-validation (*GCV*): The GCV criterion is based on the fact that a good parameter must predict the missing data well [12,21]. Its principle is:

- one determines $F_{\alpha,j}$, the solution obtained when one uses the whole data except the j component of $[\mathbf{S}]$; $F_{\alpha,j}$ is then the solution of the following problem:

$$\min_F \left\{ \sum_{i=1,\ i\neq j}^{n} |\mathbf{S}_i - (\mathbf{GF})_i|^2 + \alpha \|\mathbf{F}\|_2^2 \right\}, \tag{22}$$

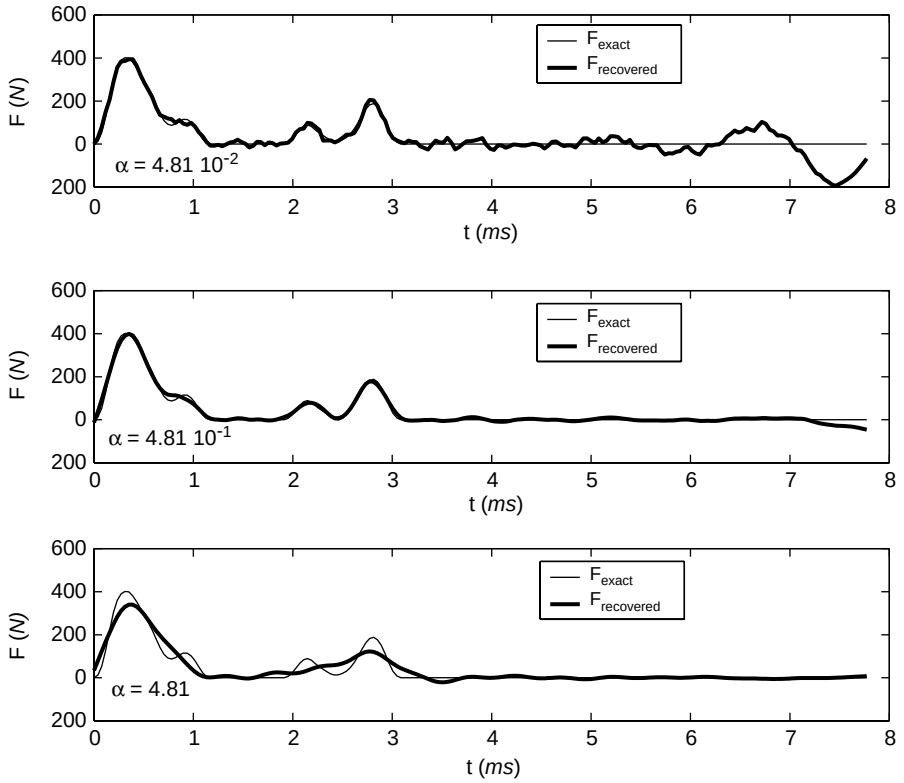

Fig. 11. Force recovered for different values of α with Tikhonov regularization.

- one predicts the unused data $\mathbf{S}_j$: $\mathbf{S}_j = (\mathbf{G}\mathbf{F}_{\alpha,j})_j$;
- the regularization parameter is the one which minimizes the predictive mean-square error; Desbat [21] has shown that comes down to minimizing the $\mathscr{G}$ function (called GCV function):

$$\mathscr{G} = \frac{\|\mathbf{G}\mathbf{F} - \mathbf{S}\|}{\|\mathbf{I}_m - \mathbf{G}\mathbf{G}^{\sharp}\|}. \tag{23}$$

In Fig. 12, such functions GCV are plotted for the Tikhonov and truncation methods: the recovered forces are then obtained (Fig. 13).

Comments: All the recovered forces are similar: in this example, all the criteria to determine the regularization parameter and all the methods are good. Nevertheless, the parameters are not exactly the same (see Table 2). Then, one can conclude that there exists a range of good values to regularize the problem.

In the previous example, the whole criteria and methods allows one to reconstruct the force: this is not always the case. Indeed, the aim of the following section is to highlight the difficulties and to define which criteria must be used.

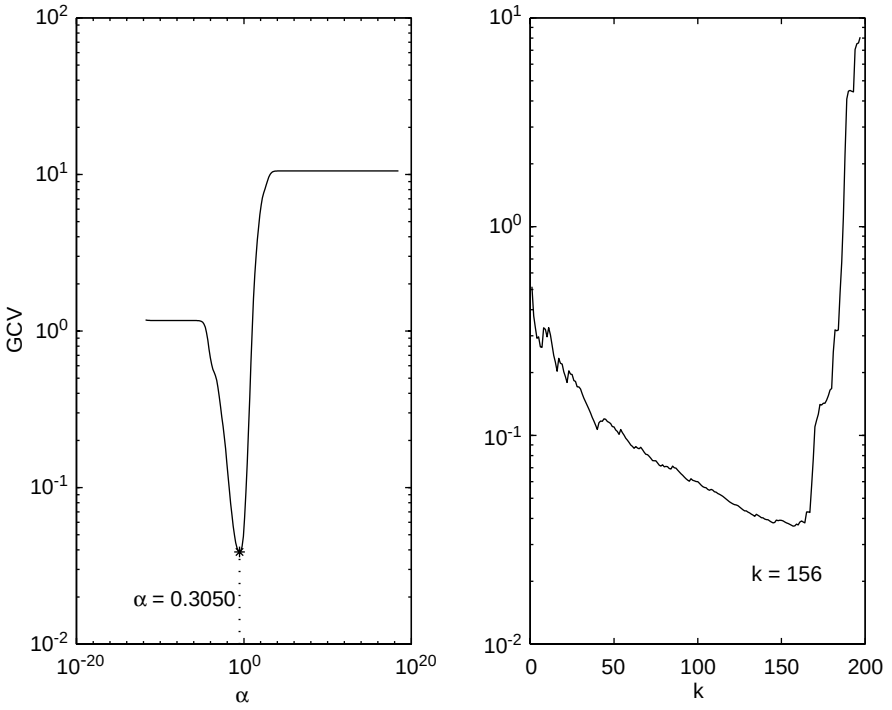

Fig. 12. GCV function for Tikhonov method and truncation method.

4.3. Experimental forces reconstruction

The methods and the criteria are now tested with the experimental data. An impact force and any force are recovered.

4.3.1. Experimental impact force

First, the L-curve (Fig. 14) is plotted. It is difficult to see the corner of this L-curve. So, as proposed in Refs. [12,18], the corner is defined as the point on the parametric L-curve:

$$(\log(||\mathbf{GF}-\mathbf{S}||_2), \log(||\mathbf{LF}||_2)) = (\log(\zeta(\alpha)), \log(\eta(\alpha))) = (\hat{\zeta}(\alpha), \hat{\eta}(\alpha)),$$

which has maximum curvature. The curvature $\kappa(\alpha)$ is defined as usual by

$$\kappa(\alpha) = \frac{(\hat{\zeta}'\hat{\eta}'' - \hat{\zeta}''\hat{\eta}')}{((\hat{\zeta}')^2 + (\hat{\eta}')^2)^{3/2}} = 2\frac{\zeta\eta}{\eta'}\frac{(\alpha^2\zeta\eta' + 2\alpha\zeta\eta + \alpha^4\eta\eta')}{(\zeta^2 + \alpha^4\eta^2)^{3/2}}$$

with

$$\eta' = -\frac{4}{\alpha}\sum_{i=1}^{n}(1-f_i)f_i^2\frac{(\mathbf{u}_i^{\mathrm{t}}\mathbf{S})^2}{\sigma_i^2}.$$

The regularization parameter is then obtained: $\alpha = 0.41$.

Table 2
Regularization parameters—numerical signals

	Tikhonov	Truncation
L-curve	0.4810	125
GCV	0.3050	156

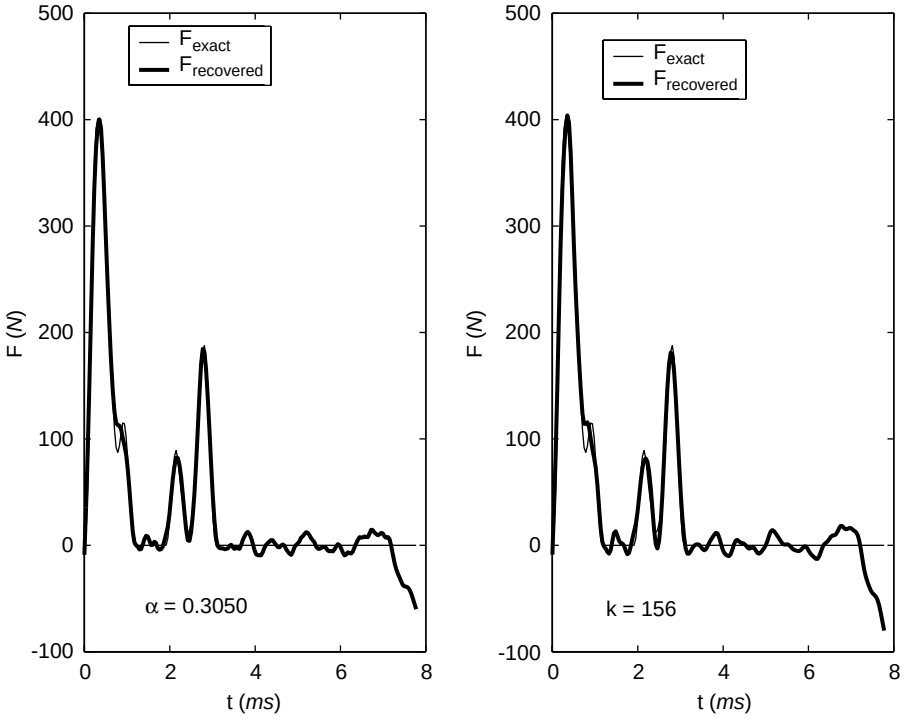

Fig. 13. Force recovered with the parameter obtained with the GCV function.

The GCV criterion is also tested, as shown in Fig. 15. For the Tikhonov method, the minimum is obtained for $\alpha = 0.034$, but the GCV function is very flat in a large range of the parameter: then it is not easy to choose a parameter.

For the truncation method, the parameter $k = 2$ is obtained: only the singular vectors which correspond to the singular values below the computer precision are eliminated; Fig. 16 shows that some too "oscillating" singular vectors are not eliminated: the solution is not regularized enough. This solution is frequently obtained, but it never corresponds to a good regularization parameter: the other part of the curve must be examined. The following local minimum is then for $k = 48$: the result is then good.

In that case, 3 criteria give a good parameter (see Table 3). But, if the GCV function does not give a good value, the problem is pointed out by the flatness of the curve near the minimum.

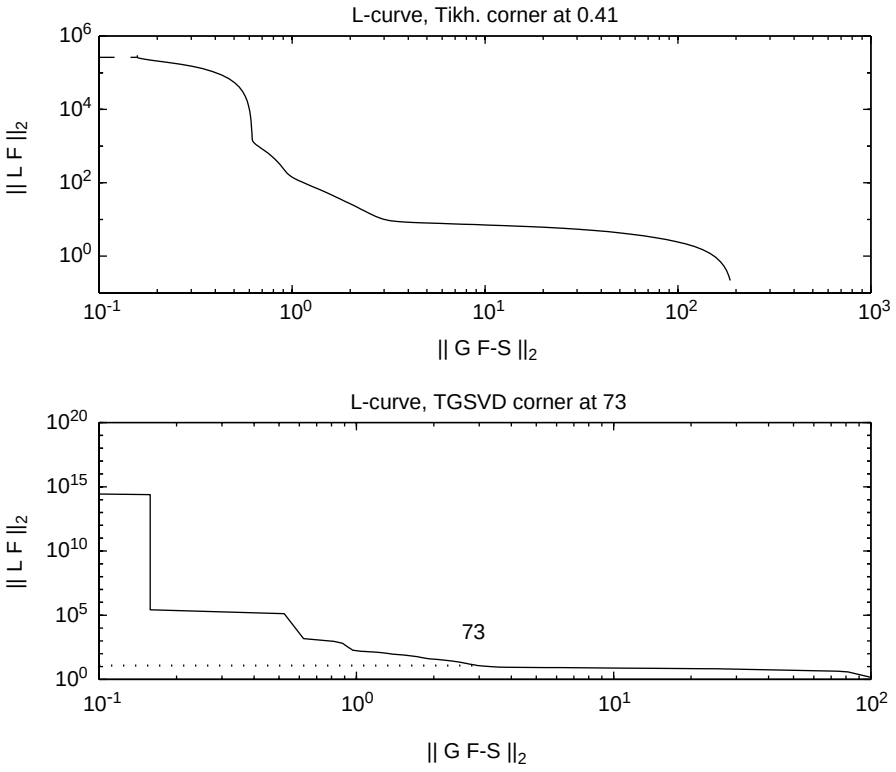

Fig. 14. L-curve $-L = D^2$—impact force.

4.3.2. Any experimental force

To test the regularization method for any force, the data shown in Fig. 17 is used.

The GCV criterion is applied for Tikhonov and truncation regularization (Fig. 18). The values obtained allow one to recover the force well, as shown in Fig. 19.

The L-curve criterion is also applied (Fig. 20). But the corners do not indicate an optimal parameter. In that case it is more interesting to use the "next" corner: it is the following local maximum of the curvature. In fact, this latter point is a real compromise: the residual norm of Eq. (2) "accepts" to increase; that was not the case with the point which has the maximum curvature (Fig, 20). The recovered force is then as good as the parameters determined with the GCV criterion, as shown in Fig. 19.

The Table 4 shows that both criteria give the same value for the regularization parameters, if the "real" corner is not used.

4.3.3. Comments

Even if for the numerical simulations all the criteria are good to determine the regularization parameter, in practice the following features must be emphasized:

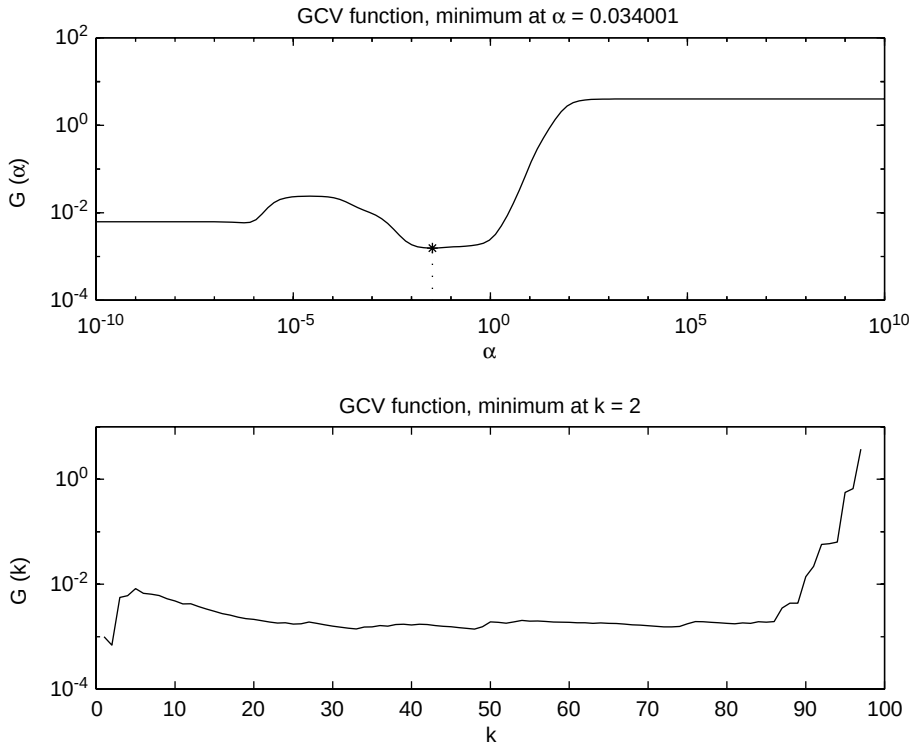

Fig. 15. GCV $-L = D^2$—impact force.

Table 3
Regularization parameters for impact force

	Tikhonov	Truncation
L-curve	0.41	73
GCV	0.034	48

- *For the truncation method*: If the criteria indicate that a few of the terms must be eliminated, the solution is never good: only the small singular values (i.e. lower than the computer precision) are eliminated; the too oscillating terms again spoil the solution.
- *For L-curve*: A real compromise must be achieved: if a corner is reached without change in the residual norm, the result is always under-regularized. The next corner gives a good value for the regularization parameter.
- *For the GCV*: If the GCV function is too flat near the minimum, the value of the regularization parameter is not reliable.

Then, the recommendation to regularize, is to use different criteria and to confront the results.

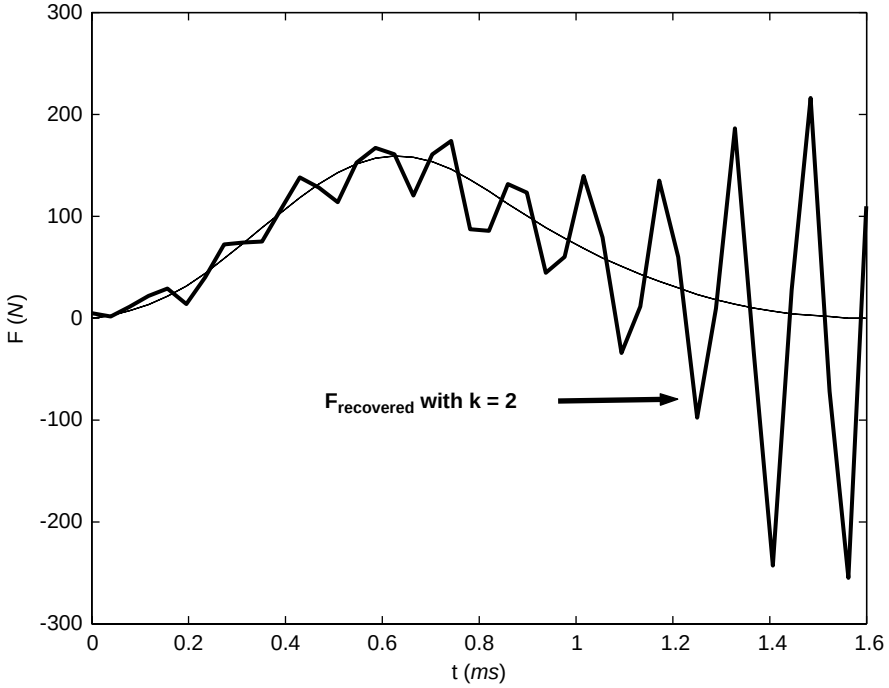

Fig. 16. GCV $-L = D^2$—under-regularized solution with truncation method.

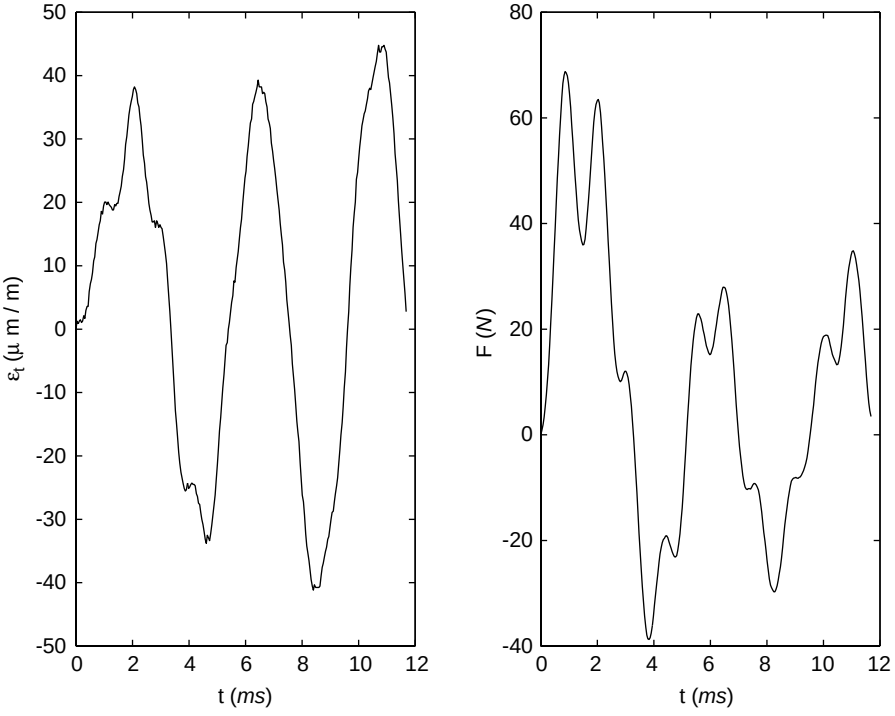

Fig. 17. Any force and its response measured at 5 cm.

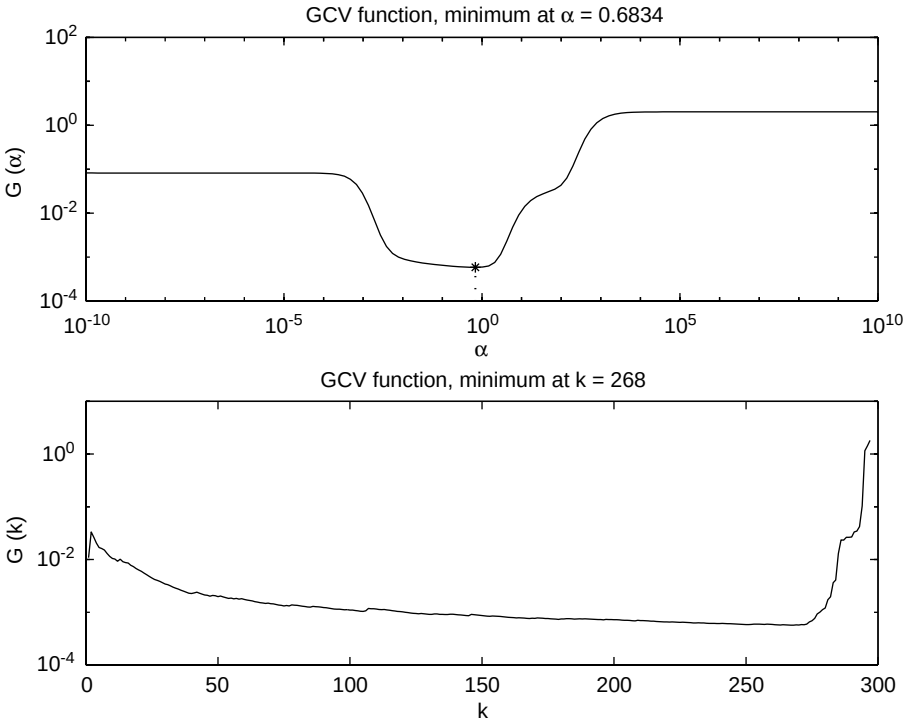

Fig. 18. GCV $-L = D^2$—any force.

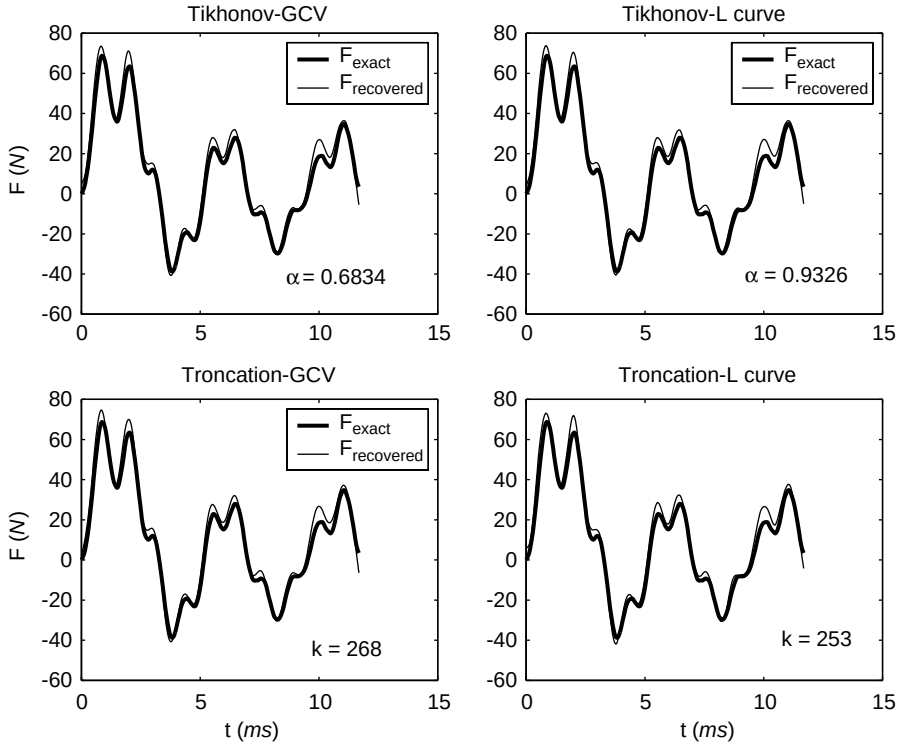

Fig. 19. Any force recovered with the different methods.

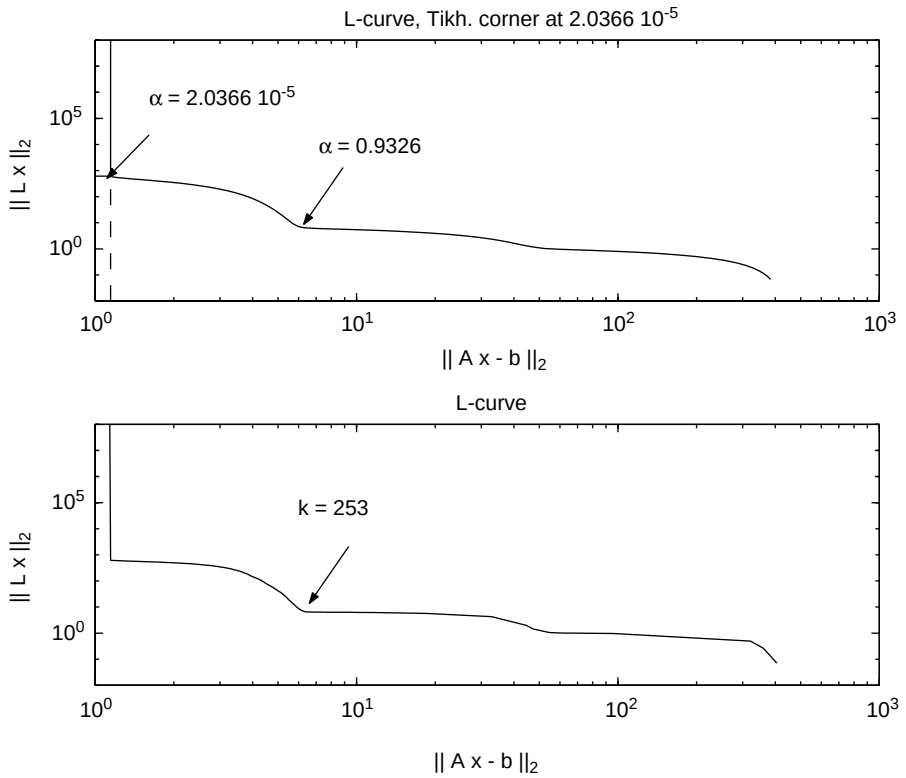

Fig. 20. L-curve $-L = D^2$—any force.

Table 4
Regularization parameters for any force

	Tikhonov	Truncation
L-curve	0.9326	253
GCV	0.6834	268

5. Conclusion

To recover an excitation by solving the algebraic system (2) is not so easy: the solution of a such system, if there exists, is not stable. This study highlights the influence of the location of the measurement point: this location modifies the condition number of the transfer matrix [**G**] and the nature of the problem. Moreover, the inverse problems are dominated by the rounding errors when the system is rank-deficient.

But, even when the system is not rank-deficient, the solution is not stable: a small measurement noise causes a severe oscillation of the solution; it is interesting to note that the results are

different if the disturbance is a modelling noise. This leads to regularize the initial problem to stabilize the solution. This consists in adding conditions to the initial problem. Some of them may be physical (non-negativity for an impact force, for example) and some others may be more abstract (''smoothness'' of the solution for example). The regularization by truncation leads to filter a signal by a low-pass filter. Then, this method would be efficient when a solution unstability is due to high frequency components. Tikhonov regularization is more global: it takes effect of the whole signal.

Those methods are more general, but involve the estimation of a regularization parameter: it is difficult to find an appropriate value even if some criteria exist. In fact, different criteria must be used: all the results obtained must be analyzed carefully and be confronted. It is worth noting that this method allows one to recover any force.

References

[1] J.F. Doyle, Further developments in determining the dynamic contact law, Experimental Mechanics 24 (4) (1984) 265–270.
[2] J.F. Doyle, Experimentally determining the contact force during the transverse impact of an orthotropic plate, Journal of Sound and Vibration 118 (3) (1987) 441–448.
[3] J.F. Doyle, Wave Propagation in Structures, Springer, Berlin, 1989.
[4] Y. Gao, R.B. Randall, Reconstruction of diesel engine cylinder pressure using a time domain smoothing technique, Mechanical Systems and Signal Processing 13 (5) (1999) 709–722.
[5] C. Chang, C.T. Sun, Determining transverse impact force on a composite laminate by signal deconvolution, Experimental Mechanics 29 (4) (1989) 414–419.
[6] C.-S. Yen, E. Wu, On the inverse problem of rectangular plates subjected to elastic impact. Part I: method development and numerical verification, Journal of Applied Mechanics 62 (3) (1995) 692–698.
[7] C.-S. Yen, E. Wu, On the inverse problem of rectangular plates subjected to elastic impact. Part II: Experimental verification and further applications, Journal of Applied Mechanics 62 (3) (1995) 699–705.
[8] H. Alison, Inverse unstable problems and some of their applications, Mathematical Scientist 4 (1979) 9–30.
[9] E. Wu, J.-C. Yeh, C.-S. Yen, Impact on composite laminated plates: an inverse method, International Journal of Impact Engineering 15 (4) (1994) 417–433.
[10] A.N. Tikhonov, V.Y. Arsenin, Solutions of Ill-posed Problems, Winston-Wiley, New York, 1977.
[11] B.A. Mair, Tikhonov regularization for finitely and infinitely smoothing operators, SIAM Journal of Mathematical Analysis 25 (1) (1994) 135–147.
[12] P.C. Hansen, Rank-Deficient and Discrete Ill-posed Problems, SIAM, Philaphedia, PA, 1998.
[13] K.F. Graff, Wave Motion in Elastic Solids, Dover Publications, New York, 1975.
[14] W.H. Press, S.A. Teukolsky, W.T. Vetterling, B.P. Flannery, Numerical Recipes, Cambridge University Press, Cambridge, 1992.
[15] Y. Qian, S.R. Swanson, A comparison of solution techniques for impact response of composite plates, Composite Structures 14 (1990) 177–192.
[16] E. Wu, T.-D. Tsai, C.-S. Yen, Two methods for determining impact-force history on elastic plates, Experimental Mechanics 35 (1992) 11–18.
[17] M.A. Branch, A. Grace, Matlab. Optimization Toolbox, The Math Works Inc., Natick, MA, 1996.
[18] T. Reginska, A regularization parameter in discrete ill-posed problems, SIAM Journal of Scientific Computing 17 (3) (1996) 740–749.
[19] S. Granger, L. Perotin, An inverse method for the identification of a distributed random excitation acting on a vibrating structure. Part I: Theory, Mechanical Systems and Signal Processing 13 (1) (1999) 53–65.

[20] L. Perotin, S. Granger, An inverse method for the identification of a distributed random excitation acting on a vibrating structure. Part II: Flox-induced vibration application, Mechanical Systems and Signal Processing 13 (1) (1999) 67–81.
[21] L. Desbat, Critères de Choix de Paramètres de Régularisation: Application à la Déconvolution, Ph.D. Thesis, Université Joseph Fourier, Grenoble, 1990.